Transport Properties of Natural Rubber Latex Layered Clay Nanocomposites

Ansu Jacob,[1] Philip Kurian,[1] Abi Santhosh Aprem[2]

[1]*Department of Polymer Science and Rubber Technology, Cochin University of Science and Technology, Kochi-22, Kerala, India*
[2]*Hindustan Latex Ltd., Akkulam, Sreekariyam P. O, Trivandrum, Kerala, India*

Received 23 January 2007; accepted 27 March 2007
DOI 10.1002/app.26615
Published online 21 February 2008 in Wiley InterScience (www.interscience.wiley.com).

ABSTRACT: Natural rubber latex layered clay nanocomposites were prepared with low loadings of nanoclay using conventional compounding technique. A higher loading of clay resulted in processing difficulties due to viscosity build up. X-ray analysis showed that nanocomposites in which layered silicate layers were either delaminated or ordered as in an intercalated structure was obtained. Partially exfoliated structure was observed from TEM photographs of nanocomposites with 3 phr nanoclay. The transport properties, sorption, diffusion, and permeation coefficients were measured using the solvent toluene at 303 K. A higher decrease for the diffusion coefficient for nanocomposites directs the presence of tortuous path for the diffusing molecules. Thermodynamic parameters show a better compatibility for the silicates with rubber resulted in the formation of an elastomeric network. Gas permeability results of the nanocomposites suggest a better barrier resistance for oxygen molecules even in lower loading of nanoclay and different gas transport models (Nielsen, Bharadwaj, Cussler) were applied to describe the behavior of these nanocomposites. © 2008 Wiley Periodicals, Inc. J Appl Polym Sci 108: 2623–2629, 2008

Key words: rubber; nanocomposites; barrier; clay; swelling

INTRODUCTION

Polymer nanocomposites are receiving a great amount of attention in science and technology because of their many applications in everyday life. As the building blocks of nanocomposites are of nanoscale they have an enormous interface area and therefore there are a lot of interface between the two intermixed phases when compared to usual microcomposites. Thus, nanocomposites exhibit new and improved performance properties in comparison with the pristine polymer. Rubber–clay nanocomposites have also drawn great attention in recent years.[1–5] A better enhancement of modulus, failure properties such as tensile and tear strength, abrasion resistance, barrier properties, swelling resistance, and thermal properties is obtained. Application of a small amount of intercalated clay to the rubber matrix can provide considerable improvement in barrier performance of various rubbers.[6] According to the free volume concept, the chain mobility provides a driving force for diffusion of small molecules. In a nanocomposite the molecular mobility is severely reduced in the close vicinities of the clay platelets and this provides a tortuous path for the permeating molecules. Transport properties are of considerable importance for latex nanocomposites as their applications mainly involves barrier materials. Not much has been done to improve the barrier performance of rubbery material although the commercialization of such nanocomposites is expected to be high in rubber industries.

The addition of any fillers usually reduces the strength of the rubber obtained from latex. But layered silicates are suitable additives for latex. A variety of clay has recently been used to obtain nanocomposites by exploiting the ability of clay layers to be dispersed into polymer at the nanoscale level. Montmorillonite (MMT) clays are relatively cheap material and fine grained particle with high surface area. They are readily dispersed in water (latex) and as easily incorporated as a dry or aqueous dispersion without risking the destabilization of the latex. The crystal structure of the clay itself is most important. In aqueous dispersion clay swells since its layers are separated by hydration, which makes its good dispersion in the rubber products. The characteristic expansion of the interlayer structure exposes a large active surface area and permits polymer molecule to enter into the galleries. Separation of clay platelets can occur under certain conditions giving very high aspect ratio filler, which dramatically improves composite properties.

Latex clay nanocomposites were prepared by coagulation method[7] and conventional compounding technique, an improvement in properties was also

Correspondence to: P. Kurian (pkurian@cusat.ac.in).

TABLE I
Recipe for Mixing

Ingredients	Mix 1 (phr)	Mix 2 (phr)	Mix 3 (phr)	Mix 4 (phr)
NR Latex (60% DRC)	100	100	100	100
Sulphur (50%)	1.5	1.5	1.5	1.5
Zinc Oxide (50%)	0.9	0.9	0.9	0.9
PotassiumOleate (10%)	0.8	0.8	0.8	0.8
Accelerator (50%)	0.7	0.7	0.7	0.7
Antioxidant (50%)	0.5	0.5	0.5	0.5
Clay dispersion (2%)	0	1	2	3

reported.[8] The aim of this work was to prepare natural rubber (NR)-latex clay nanocomposites by conventional compounding method and to investigate the effect of the percentage of clay on their transport properties.

EXPERIMENTAL

Materials

Sodium montmorillonite clay (cloisite Na^+), which has an ion exchange capacity of 92.6 mequiv./100 g clay and an interlayer distance of 11.7 Å, used for the study was obtained from Southern Clay Products, USA. Double centrifuged latex used for compounding was obtained from local suppliers. Compounding ingredients like sulfur, accelerators, antioxidant, activators, etc. used were of commercial grade.

Preparation of natural rubber latex–clay nanocomposites

Aqueous dispersion (2%) of layered clays was prepared by means of an ultrasonic stirrer (Oscar ultrasonics) and other compounding ingredients were prepared by ball milling. The compounding recipe is given in Table I. After compounding, the latex is kept for five days for maturation. Continuous slow stirring was maintained during this time. The compounded latex after removing the dirt and coarse particles by filtering through sieve is then casted on raised glass plate having a dimension of 13 cm × 10 cm × 1 mm, the casting was then allowed to dry in air till becomes transparent, and then vulcanized at 343 K for 4 h in an air circulated oven.

Characterization using X-ray diffraction technique

X-ray diffraction (XRD) was used to study the nature and extend of dispersion of the clay in the filled sample. XRD were collected using Bruker, D_8 Advance diffractometre at the wavelength Cu Kα = 1.54 Å, a tube voltage of 40 kV and tube current of 25 mA. Bragg's law defined as $n\lambda = 2d \sin\theta$, was used to compute the crystallographic spacing (d) for the clay.[9] The samples were scanned in step mode by 1.0°/min, scan rate in the range of 2–13°.

Transmission electron microscopy

The transmission electron microscopy was performed using a JEOL JEM-2010 (Japan) transmission electron microscope, operating at an accelerating voltage of 200 kV. The samples for TEM analysis were prepared by ultra-cryomicrotomy using a Leica Ultracut UCT. Freshly sharpened glass knives with cutting edge of 45° were used to get the cryosections of 50–70 nm thickness. Since these samples were elastomeric in nature, the temperature during ultra cryomicrotomy was kept at −50°C. The cryosections were collected individually on sucrose solution and directly supported on a copper grid of 300-mesh size.

Swelling studies

A circular specimen of 0.2 cm diameter and 1 mm thickness were cut using a sharp edged circular disc from the vulcanized samples. The samples were immersed in airtight test bottles containing about 15–20 mL of toluene maintained at constant temperature. Samples were removed periodically and the surface adhered solvent drops were wiped off carefully by pressing them between filter wraps. The mass of the sorbed sample was determined immediately on a digital balance with an accuracy of ±0.01 mg. As the weighing was done within 30–40 s, the error due to evaporation of other than surface adsorbed liquid is considered insignificant. Desorbed weights of the samples were also taken after complete removal of the solvent.

Gas permeability testing

The air permeability of the latex layered silicate membranes were measured using Lyssy Manometric Gas Permeability Tester L100-2402. The test gas used was oxygen at a rate of 500 mL/min. Permeability of the samples is calculated using the equation, $P_m = (T_r \times P_r)/t_m$, where P_m is the permeability of the test sample, t_m is the interval time constant for the

test sample, P_r is the permeability of the reference (standard PET sample), and T_r is the interval time constant for standard PET. The test was conducted at a temperature of (25 ± 1)°C and a relative humidity of 65 ± 0.5.

RESULTS AND DISCUSSION

XRD studies

XRD is widely used to understand whether a true nanocomposites has been formed or not. If the crystalline order is manifested as a peak corresponding to the same basal spacing as in the pristine clay, then we have a conventional composite. Appearance of peak at lower angle corresponding to higher basal spacing indicates intercalated nanocomposites. Figure 1 shows the X-ray analysis data of (a) nanoclay (cloisite Na^+) and rubber–clay nanocomposite (b). The clay showed d_{001} peak at $2\theta = 7.1°$, which corresponds to d_{001} spacing 12.35 Å and for the nanocomposites a peak at $2\theta = 3.07°$ and a shoulder one at $2\theta = 5.88°$ corresponds to interlayer distance of 28.74 and 14.99 Å respectively are seen. Both the peaks get shifted to a lower 2θ value/higher d_{001} spacing supports the idea that natural rubber (NR) latex molecules penetrate between the silicate layers. The more intense peak d_{001} spacing value increased by 16.39 Å suggests the formation of an intercalated nanocomposites.

Transmission electron microscopy

TEM was used to visualize the morphology of the clay layers in the nanocomposites. Figure 2 shows TEM micrographs for samples with 3 phr nanoclay. Even though XRD indicated all intercalated structures, exfoliated layers can also be observed in the TEM pictures.

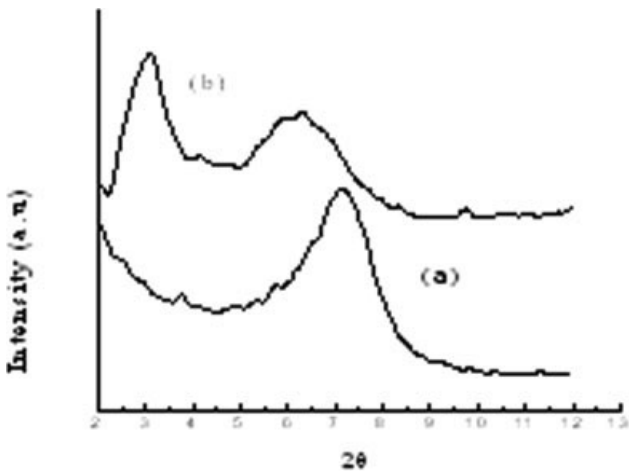

Figure 1 XRD spectrum of (a) nanoclay and (b) nanocomposite with 1 phr clay.

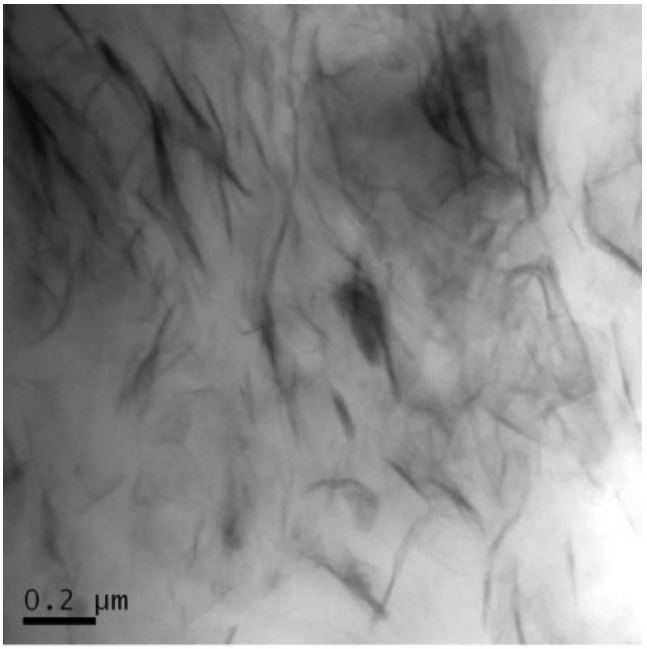

(a)

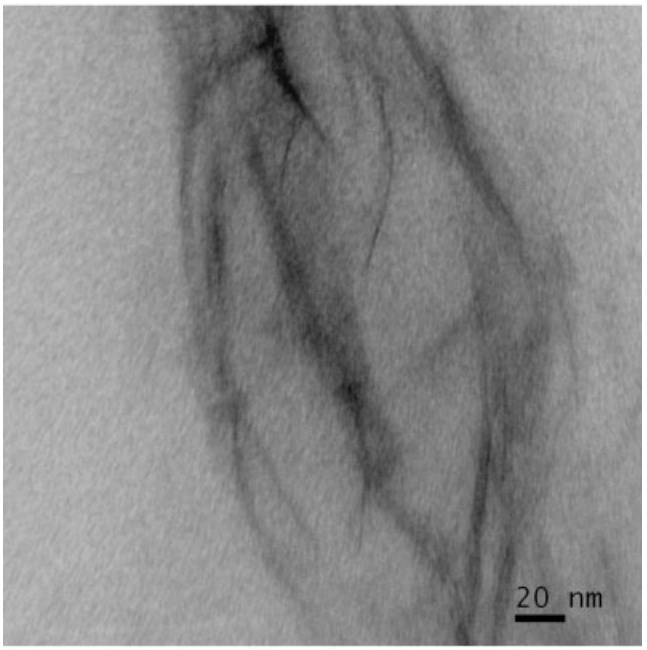

(b)

Figure 2 TEM micrographs of nanocomposite with 3 phr nanoclay (a) at low magnification and (b) at higher magnification.

Swelling studies

The mole percent uptake of the sample is calculated from the diffusion data. The Q_t values were determined as

$$Q_t = \frac{(\text{Wt of the solvent sorbed at a given time})/(\text{Mol wt of the solvent})}{(\text{Initial wt of the rubber specimen} \times 100)}$$

At equilibrium swelling, Q_t becomes Q_∞. Sorption curves of the vulcanisates which are obtained by plotting Q_t (mole% uptake per 100 g of the solvent) against time are shown in Figure 3. For all compositions, the uptake is rapid in the initial zone. After this, the sorption rate decreases, leading to a plateau corresponding to equilibrium swelling. Note that the gum has maximum toluene uptake at equilibrium swelling. The swelling of the material is strongly reduced in the presence of clay within the NR matrix. The presence of impermeable clay layers decreases the rate of transport by increasing the average diffusion path length in the specimen. To determine how the clay content affects the permeability, we measured the transport properties of the samples.

The mechanism of diffusion was investigated using the equation[10–12]

$$\log\ Q_t/Q_\infty = \log k + n \log t$$

The value of k depends on the structural features of polymer, whereas the value of n determines diffusion mechanism. For the Fickian mode, case 1, the value of n is 0.5 and it occurs when the rate of diffusion of penetrant molecules is much less than the relaxation rate of the polymer chains. For case 2 or non-Fickian transport, where the n value is 1, the diffusion is rapid when compared with the simultaneous relaxation process. However, in the case of anomalous transport where the n value is in between 0.5 and 1, both solvent diffusion and polymer relaxation rate are comparable. The values of n and k are given in Table II. In this study, it is seen that with increase in clay content, anomalous mechanism shifts to the Fickian mode.

The polymer swelling is also affected by solvent transport. As swelling increases, free volume

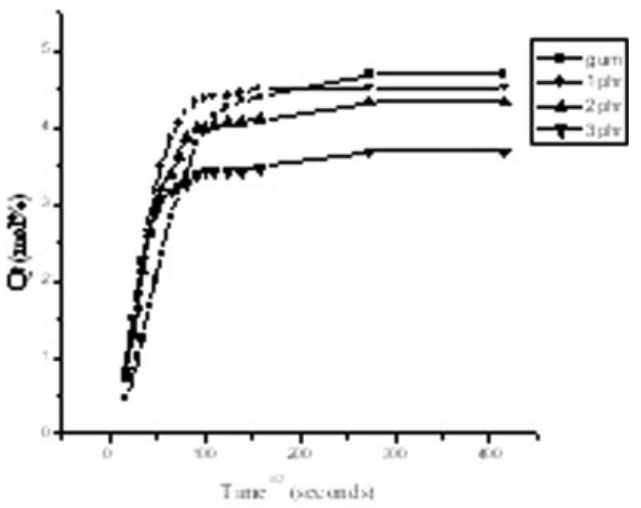

Figure 3 Swelling behavior of the NR latex samples in toluene at 303 K.

TABLE II
Variation in n and k Values with Loading of Nanoclay

Samples	n	k
Mix 1	0.6679	−1.4621
Mix 2	0.6647	−1.2099
Mix 3	0.5038	−1.1144
Mix 4	0.4792	−0.9262

increases because of chain mobility, which facilitates transport process. The diffusion coefficient can be determined using the relation[13,14]

$$D = \pi\left[\frac{h\theta}{4Q\infty}\right]^2$$

where h is the initial thickness of rubber sample, θ the slope of the linear portion of the sorption curve Q_t versus $t^{[1/2]}$ (Fig. 3). The values of D are given in the Table III. The variation of D depends on the solvent uptake, which is maximum for the gum vulcanizate. Adding clay within the NR matrix results in a progressive decrease of D value and a substantial decrease with increase in clay content. This may be due to the reduced availability of space for solvent molecules in the intercalated structure of the nanocomposites. This also shows the strong interaction between the filler and the matrix, which limits the toluene diffusivity within the entangled polymer matrix.

The permeation of a solvent into a polymer membrane will also depend on the sorptivity of the penetrant in the membrane. Hence, sorption coefficient S has been calculated using the relation.[15]

$$S = \frac{W_S}{W}$$

Where W_s is the weight of the solvent at equilibrium swelling and W, the initial weight of the polymer sample. The numerical values of sorption coefficient are also given in Table III. The values are slightly higher in the gum than in the nanocomposites because of the higher contribution of the layered silicates.

Since the permeability depends on both diffusivity and sorptivity, the permeation coefficient has been determined using the relation[15]

TABLE III
Variation of Diffusion Coefficient (D), Sorption Coefficient (S), and Permeation Coefficient (P) with Loading of Nanoclay

Samples	$D \times 10^{-}$ (cm^2/s)	S	$P \times 10^{-6}$ (cm^2/s)
Mix 1	7.12	4.31	3.08
Mix 2	6.22	4.15	2.58
Mix 3	4.22	3.33	1.43
Mix 4	4.20	3.39	1.40

TABLE IV
Variation in Crosslink Density and Molar Mass Between Crosslinks with Loading of Nanoclay

Samples	Crosslink density, υ (mol/g) $\times 10^{-5}$	Molar mass between crosslinks, M_c (g/mol)
Mix 1	4.25	11,764.71
Mix 2	4.46	11,210.76
Mix 3	5.83	8576.329
Mix 4	7.61	6570.302

$$P = D \times S$$

The permeability coefficient, the net effect of sorption, and diffusion process is also found to be decreasing. The values obtained for P are given in the Table III. It is seen that the decreasing value of the permeability of the nanocomposites is largely dominated by the diffusion phenomenon, as shown by the respective values of sorption and diffusion reported in the Table III.

As diffusion is influenced by polymer morphology, the molar mass between crosslinks M_c from the sorption data is also determined. The rubber solvent interaction parameter, which is needed for the estimation, has been calculated using the equation[15]

$$\chi = \beta + \frac{V_S}{RT}(\partial s - \partial p)^2$$

where V_s is the molar volume of the solvent ∂s and ∂p are solubility parameters of solvent and polymer taken from the polymer handbook. R is the universal gas constant and T the absolute temperature, β is the lattice constant and is 0.38 in this calculation.

Using χ values the molar mass between crosslinks (M_c) of the polymer was estimated from the Flory Rehner equation[16,17]

$$M_c = \frac{-\rho_p V_S (V_r)^{1/3} \chi}{\ln(1 - V_r) + (V_r) + \chi(V_r)^2}$$

where ρ_p is the density of the polymer, V_r is the volume fraction of swollen polymer, V_s is the molar volume of the solvent, and χ the interaction parameter.

The volume fraction of the polymer calculated using the equation[18]

$$V_r = \frac{(d - fw)\rho_p^{-1}}{(d - fw)\rho_p^{-1} + A_o \rho_s^{-1}}$$

where d is the desorbed weight of the polymer, f, the weight percent of filler, w, the initial weight of the polymer, ρ_p andρ_s, the density of polymer and the solvent respectively and A_0, the net solvent uptake of the polymer. The monomeric molecular weight of NR being 68 g/mol, the average number of monomeric units between crosslinks can be calculated. A decrease in the value is observed. Using the M_c values crosslink density can be calculated using the equation $\upsilon = 1/2M_c$ and is given in the Table IV.

Thermodynamic effects occurring during swelling of the elastomers chains were also analyzed. The thermodynamic approach is of great importance for understanding the rubber–filler interaction in the nanocomposites. Swelling of a sample depends on the crosslink density and the solvent used. The expansion of the rubber in the presence of a solvent will significantly modify the conformational entropy (ΔS) and the elastic Gibbs free energy (ΔG). The elastic gibbs free energy can be determined from the Flory-Huggins equation[19]

$$\Delta G = RT\left[\ln(1 - V_r) + (V_r) + \chi(V_r)^2\right]$$

And from the statistical theory of rubber elasticity, ΔS can be obtained from $\Delta G = -T\Delta S$, which assumes that no change in internal energy of the network occurs upon stretching. Both thermodynamical parameters, ΔS and ΔG, of the studied material are reported in Table V. It should be noted that ΔG increases in the presence of clay. It is assumed that ΔG is closely related to the elastic behavior of the material. i.e., the nanocomposites shows a better elasticity than the gum compound and it increases with increase in clay content These results can be attributed to better compatibility between the silicate and rubber, the rubber molecules can penetrate into the galleries more easily, giving rise to a process of exfoliation of the silicate layer. This exfoliation is responsible for the noticeable increase of entropy as compared with gum.

Gas permeability testing

The oxygen permeability of the nanoclay filled and gum vulcanisate having 1 mm thickness are depicted in Figure 4. It is clearly seen that the oxygen permeability decreased substantially (66%) by incorporation of 1 phr of layered silicate. As the silicate loading was increased to 3 phr, only a slight improvement in permeation resistance was observed.

Gas barrier in plate like particle filled polymer nanocomposites was traditionally explained in terms of Nielson model, originally adopted to describe the

TABLE V
Thermodynamical Parameters ΔG and ΔS of the Compounds

Samples	ΔG (J/mol)	ΔS (J/mol) $\times 10^{-2}$
Mix 1	−10.61	3.50
Mix 2	−11.17	3.68
Mix 3	−15.21	5.00
Mix 4	−20.66	6.82

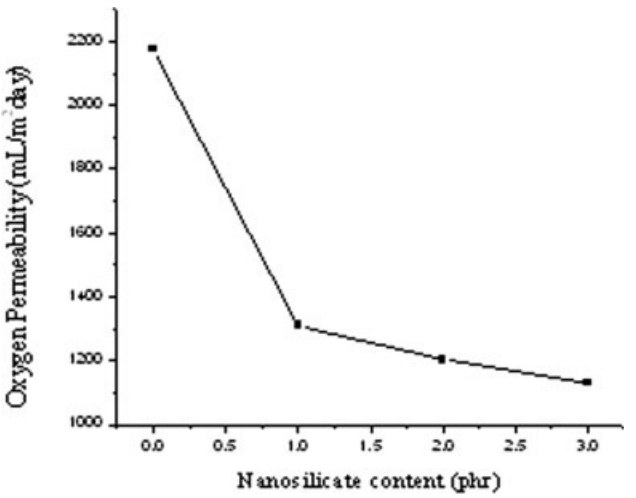

Figure 4 Oxygen permeability of the NR latex films having 1 mm thickness.

tortuousity effect of plate like particulates on gas permeability of polymer composite structures.[20] This model system consisting of uniform platelets homogeneously dispersed in the polymer matrix and oriented parallel to the polymer film surface. The model can be applied using the equation,

$$\frac{P}{P_0} = \frac{1-\phi_f}{1+\frac{L}{2W}\phi_f}$$

to obtain the clay aspect ratio from the permeability data of these nanocomposites. In the equation, P is the permeability of the nanocomposite, P_0 is the permeability of the gum vulcanizate, and ϕ_f is the volume fraction of the clay. L and W are length and width of the clay sheets, respectively, its ratio L/W, defines the aspect ratio α, of the fillers. The model assumes that the fillers are impermeable to the diffusing gas or liquid molecule, and are oriented perpendicularly to the diffusion direction. Thus, the presence of the filler particles creates tortuous path for the permeant to travel through the composites. The denominator on the right hand side of the equation is also referred to as the tortuousity factor, τ, defined as the distance a molecule must travel to get through the film divided by the thickness of the film. With the increase in clay content it is seen that the aspect ratio is decreasing (Table VI) and thus the tortuousity factor increases. Permeability data (Fig. 4) of the nanocomposites also suggests the same and thus the permeation of oxygen molecules through the nanocomposites fits with Nielsen model. Sample with lower clay content presented the higher aspect ratio due to the better dispersion of clay in the rubber matrix, thus only a slight decrease in the permeability is observed with the increase in clay content.

Bharadwaj[21] modified Nielson model to incorporate an orientation parameter S, in which a range of relative orientations of the clay sheets with respect to each other

$$\frac{P}{P_0} = \frac{1-\phi_f}{1+\frac{L}{2W}\phi_f\left(\frac{2}{3}\right)\left(S+\frac{1}{2}\right)}$$

represented by θ (the angle between the direction of preferred orientation and the sheet normal) could be applied. Bharadwaj's expression is shown in the equation accompanied by orientation parameter equation

$$S = \frac{1}{2}\left(3\cos^2\theta - 1\right)$$

In the case of random platelet orientation ($S = 0$), the tortuousity decreases with orientation and diffusion is facilitated as opposed to parallel orientation ($S = 1$ or Nielson model). This model predicts higher aspect ratios for the nanocomposites than the Nielson's model. Moreover, in the case of this latex nanocomposites prepared by the solution casting method, majority of the clay layers orient in the same direction rather than randomly due to the small restriction for the mobility of clay layers in the latex. Thus, the Bharadwaj model cannot be applied to the latex nanocomposite.

Another model used to describe gas behavior through a membrane was developed by Cussler et al.[22] with focus on the diffusion of a small gas molecule through a matrix partly filled with impermeable flakes. The flakes are oriented perpendicular to the direction of diffusion and have one very long dimension so that the diffusion is essentially two dimensional. The diffusion is mainly related to three factors: the tortuous wiggles to get around the flakes, the tight slits between the flakes, and the resistance of going from the wiggle to the slit. The model assumes that the diffusion depends on the aspect ratio and volume fraction of the impermeable filler.

$$\frac{D}{D_0} = \frac{1}{1+\frac{(L/2W)^2\phi_f{}^2}{(1-\phi_f)}}$$

TABLE VI
Aspect Ratio of Clay from Permeability Studies

	Aspect ratio		
Samples	Nielsen's Model	Bharadwaj's Model	Cussler's Model
Mix 2	129.04	387.12	159.84
Mix 3	77.34	232.02	87.06
Mix 4	57.80	122.38	61.14

where D is the diffusion coefficient of the composites, D_0 is the diffusion coefficient of the pure polymer.

A permeability model can be obtained by multiplying the diffusion by the appropriate solubility. Since the model assumes linear relationship between solubility of filled composites and volume fraction, $S = S_0 (1 - \phi_f)$, where S is the solubility of the filled composites and S_0 is the solubility of pure polymer. The permeability expression is the following.

$$\frac{P}{P_0} = \frac{(1 - \phi_f)^2}{1 - \phi_f + (L/2W)^2 \phi_f^2}$$

The aspect ratio calculated using the Cussler model is much higher than that calculated from the Nielsen model. For the nanocomposites with this very low clay loading a better homogeneous dispersion is achieved and thus this model cannot be applicable for latex nanocomposite.

CONCLUSIONS

Natural rubber latex–clay nanocomposites were prepared with low-level of clay loading using conventional compounding technique. Even though XRD indicated all intercalated structures, exfoliated layers can also be observed in the TEM pictures. Transport properties of the nanocomposites were studied in detail. The sorption, diffusion, and permeation coefficients were measured using toluene at 303 K. Because of the tortuous path available for the solvent molecule in the intercalated nanocomposites a considerable decrease in diffusion, permeation and sorption coefficients were observed. It was observed that the decreasing value of the permeability of the nanocomposites was largely dominated by the diffusion phenomenon. The permeation resistance of the nanocomposite was confirmed by the gas permeability testing and it fits with the Nielson's model, which describes the tortuousity effect of plate like particulates on gas permeability of polymer composite structures. Oxygen permeability of the natural rubber latex film is decreased by 66% with 1 phr of nanoclay loading. The thermodynamical parameters ΔS and ΔG direct the formation of a better elastic and exfoliated nanocomposite. As the barrier properties of latex films have a prominent role in dipped goods, it has high potential for commercialization.

References

1. Mousa, A.; Karger K. J Macromol Mater Eng 2001, 54, 166.
2. Peter, C.; Lebron, N.; Thomas, J.; Pinnavaia, T. J Chem Technol 2001, 13, 3760.
3. Wang, Y.; Zhang, L.; Tang, C.; Yu, D. J Appl Polym Sci 2000, 78, 1879.
4. Nair, G. K.; Dufresne, A. Biomacromolecules 2003, 4, 666.
5. Arroyo, M.; Manchado, L. M. A.; Herroro, B. Polymer 2003, 44, 2447.
6. Hanser. In Engineering with Rubber: How to Design Rubber Components; Gent, A. N., Ed.; 1992; Chapter 182.
7. Wu, P. Y.; Zhang, L. Q.; Wang, Y. Q.; Yiliang; Yu, D. S. J Appl Polym Sci 2001, 82, 2842.
8. Varghese, S.; Karger Kosis, J. Polymer 2003, 44, 4921.
9. Sperling, L. H. Introduction to Physical Polymer Science, 2nd ed.; Wiley: USA, 2001; p 204.
10. Aithal, U. S.; Aminabhavi, T. M.; Cassidy, P. E. J Membr Sci 1990, 50, 22.
11. Franson, N. M.; Peppas, N. A. J Appl Polym Sci 1983, 28, 1299.
12. Chiou, J. S.; Paul, D. R. Polym Eng Sci 1986, 26, 1228.
13. Crank, J. The Mathematics of Diffusion, 2nd ed.; Oxford: Clarendon Press, 1975; p 244.
14. Britton, L. N.; Ashman, R. B.; Aminabhavi, T. M.; Cassidy, P. E. J Chem Educ 1988, 65, 368.
15. Aprem, A. S.; Joseph, K.; Mathew, A. P.; Thomas, S. J Appl Polym Sci 2000, 78, 941.
16. Khinnava, R. S.; Aminabhavi, T. M. J Appl Polym Sci 1991, 42, 2321.
17. Flory, P. J.; Rener, Jr. J Chem Phys 1943, 11, 521.
18. Cassidy, P. E.; Aminabhavi, T. M.; Thompson, C. M. Rubber Chem Tech 1983, 56, 594.
19. Kojima, Y.; Usuki, A.; Kawasumi, M.; Okada, A.; Fukushima, Y.; Kurauchi, T.; Kamigaito, O. J. Mater Res 1993, 8, 1174.
20. Nielsen, L. J Macromol Sci Chem 1967, A1, 929.
21. Bharadwaj, R. Macromolecules 2001, 34, 9189.
22. Cussler, E.; Hughes, S.; Ward, W., III; Aris, R. J Membr Sci 1998, 38, 161.